Molecular Biology of the Cell
Vol. 8, 663–673, April 1997

Differential Localization of Myosin and Myosin Phosphatase Subunits in Smooth Muscle Cells and Migrating Fibroblasts

Kohei Murata,* Katsuya Hirano,† Emma Villa-Moruzzi,‡ David J. Hartshorne,† and David L. Brautigan*§

*Center for Cell Signaling, University of Virginia Health Sciences Center, Charlottesville, Virginia 22908; †Muscle Biology Group, University of Arizona, Tucson, Arizona 85721; and ‡Department of Biomedicine, University of Pisa, Pisa, Italy

Submitted September 3, 1996; Accepted January 28, 1997
Monitoring Editor: Tom Pollard

Myosin II light chains (MLC20) are phosphorylated by a Ca^{2+}/calmodulin-activated kinase and dephosphorylated by a phosphatase that has been purified as a trimer containing the δ isoform of type 1 catalytic subunit (PP1Cδ), a myosin-binding 130-kDa subunit (M130) and a 20-kDa subunit. The distribution of M130 and PP1C as well as myosin II was examined in smooth muscle cells and fibroblasts by immunofluorescence microscopy and immunoblotting after differential extraction. Myosin and M130 colocalized with actin stress fibers in permeabilized cells. However, in nonpermeabilized cells the staining for myosin and M130 was different, with myosin mostly at the periphery of the cell and the M130 appearing diffusely throughout the cytoplasm. Accordingly, most M130 was recovered in a soluble fraction during permeabilization of cells, but the conditions used affected the solubility of both M130 and myosin. The PP1Cα isoform colocalized with M130 and also was in the nucleus, whereas the PP1Cδ isoform was localized prominently in the nucleus and in focal adhesions. In migrating cells, M130 concentrated in the tailing edge and was depleted from the leading half of the cell, where double staining showed myosin II was present. Because the tailing edge of migrating cells is known to contain phosphorylated myosin, inhibition of myosin LC20 phosphatase, probably by phosphorylation of the M130 subunit, may be required for cell migration.

INTRODUCTION

Actomyosin is the molecular motor responsible for contractility of muscle and migration of cells (Lauffenburger and Horwitz, 1996). The activity of actin-activated Mg-ATPase of myosin II is regulated by phosphorylation of the myosin regulatory light chain (MLC20)[1] in smooth muscle and nonmuscle cells (Somlyo and Somlyo, 1994). Phosphorylation at serine 19 and threonine 18 is catalyzed by myosin light chain kinase (MLCK), which is activated by calmodulin and Ca^{2+}. Dephosphorylation is catalyzed by a myosin-associated type 1 protein phosphatase, first prepared and studied about a decade ago. However, only recently has the intact myosin LC phosphatase (MLCP) been purified and its regulation investigated. A MLCP heterotrimer consisting of 130-kDa (M130), 20-kDa, and 37-kDa proteins was purified from smooth muscle myofibrils. The MLCP bound to myofibrils and was solubilized along with myosin by 0.5–0.6 M NaCl. The 37-kDa protein turned out to be the δ isoform of the type 1 catalytic subunit (PP1C). M130 and 20-kDa proteins were novel proteins. The cDNA for regulatory subunits of smooth muscle MLCP have been

§ Corresponding author.

[1] Abbreviations used: CEF, chicken embryo fibroblast; FAK, focal adhesion kinase; M130, 130-kDa subunit of MLCP; MLC20, 20-kDa myosin regulatory light chain; MLCK, myosin light chain kinase; MLCP, myosin LC20 phosphatase; PP1C, catalytic subunit of type 1 protein phosphatase; SMC, smooth muscle cell.

© 1997 by The American Society for Cell Biology

cloned (Chen *et al.*, 1994a; Shimizu *et al.*, 1994; Shirazi *et al.*, 1994). The M130 was detected in other tissues using a monoclonal antibody; therefore, this type of phosphatase probably reacts with myosin in a variety of cell types (Okubo *et al.*, 1994).

It has been suggested that the trimeric MLCP is regulated by arachidonic acid-induced dissociation of the catalytic subunit (Gong *et al.*, 1992) or by phosphorylation of its M130 subunit (Ichikawa *et al.*, 1996b). Reports of rho-dependent regulation of MLCP activity implicate the phosphatase as an important partner in physiological control of MLC20 phosphorylation (Hirata *et al.*, 1992; Gong *et al.*, 1996; Kimura *et al.*, 1996). The M130 and PP1C, but not the 20-kDa subunit of MLCP, also have been purified by affinity chromatography on rhoA-GTP (Kimura *et al.*, 1996). The results show that M130 binds both myosin and rhoA. However, the subcellular localization of MLCP in smooth muscle or non-smooth muscle cells has not been investigated.

Cellular motility and cytoskeletal organization of nonmuscle cells involve regulated phosphorylation of MLC20. Microinjection of exogenous PP1C, but not protein phosphatase 2A catalytic subunit, dephosphorylated MLC20 in cultured fibroblasts and reorganized the actin microfilaments (Fernandez *et al.*, 1990). Migration of fibroblasts has been studied with a wound-healing model (Conrad *et al.*, 1993). Localization of different myosins in migrating cells showed myosin I was mainly located in lamellipodia and presumably involved in protrusion. Phosphorylated myosin II was concentrated on the tailing edge of migrating cells and presumably was generating a contractile force to pull the integrins from the extracellular matrix in the process of detachment (for reviews, Huttenlocher *et al.*, 1995; Lauffenburger and Horwitz, 1996). It has been suggested that MLCK is activated on the tailing edge to keep cells migrating forward, which agrees with evidence that the Ca^{2+} level is elevated on the tailing edge. One hypothesis for regulating phosphorylation of myosin II on the tailing edge of migrating cells would be selective localization of MLCP to exclude it from this region. In this study, we used immunofluorescence microscopy and Western blotting of subcellular fractions to examine distribution of myosin and M130, plus PP1Cα and PP1Cδ in fibroblasts, smooth muscle cells (SMCs) and migrating cells in a wound-healing model.

MATERIALS AND METHODS

Antibody Reagents and Western Blotting Analysis

Monoclonal antibody for M130 was made as described before (Trinkle-Mulcahy *et al.*, 1995). Rabbit polyclonal antibody against M130 was made against a recombinant protein encoding 1–674 of M130 (Ichikawa *et al.*, 1996b) and purified through DEAE Affi-gel blue (Bio-Rad, Hercules, CA). This purified antibody was kindly provided by Dr. Masaaki Ito (Mie University, Tsu, Japan). Monoclonal antibody raised against chicken gizzard myosin (Ito *et al.*, 1989) recognized the S2 region of the myosin heavy chain. Sheep polyclonal antibody against MLCK was made against purified chicken MLCK and affinity purified with a MLCK column. Affinity-purified rabbit polyclonal antibody against C-terminal peptide of human PP1Cα (GRPITPPRNSAKAKK) was purchased from Upstate Biotechnology (Lake Placid, NY). Affinity-purified rabbit anti-PP1Cδ polyclonal antibody was made against C-terminal peptide (TPPRTANPPKKR) of rat PP1Cδ (Villa-Moruzzi *et al.*, 1996). Monoclonal antibody against focal adhesion kinase (FAK) was kindly donated by Dr. J. Thomas Parsons (University of Virginia, Charlottesville, VA).

Chicken embryo fibroblasts (CEFs) were provided by Dr. J. Thomas Parsons (University of Virginia). Rat aortic SMCs were provided by Dr. Gary Owens (University of Virginia). For immunoblotting to test specificity of the antibodies, cells were scraped from 100-mm dishes with 0.3% Triton X-100 in TBS (25 mM Tris-HCl, pH 7.4, 150 mM NaCl) containing 10 μg/ml leupeptin, 10 μg/ml aprotinin, and 1 mM phenylmethylsulfonyl fluoride (PMSF). Cell lysates were collected and the total protein was precipitated with −20°C acetone, recovered by centrifugation, and dissolved with Laemmli sample buffer containing 6 M urea. Samples were boiled for 5 min and analyzed by SDS-PAGE. Proteins were transferred to nitrocellulose membranes and Western blotting was performed using horseradish peroxidase-conjugated secondary antibody (Pierce, Rockford, IL) and Renaissance system (DuPont NEN, Boston, MA).

Cell Culture

Cells were all maintained in plastic culture dishes at 37°C in a humidified atmosphere of 95% air/5% CO_2. CEFs were seeded in DMEM containing 10% fetal bovine serum, 1% chicken serum, and 1% penicillin/streptomycin. CEFs were used within 2 wk after harvesting (passages 1–4). SMCs were cultured in F12/DMEM containing 2 mM glutamine and 1% penicillin/streptomycin supplemented with 10% fetal bovine serum. SMCs were used at passages 5–20. The wound-healing model using CEF cells was performed according to a published protocol (Conrad *et al.*, 1993), with slight modification. In brief, cells were seeded onto a fibrinogen-coated coverglass and grown to 80–90% confluency. Then cells on half of the coverslip were scraped off with a rubber policemen and the medium was replaced. After 14–16 h, medium was removed and cells were fixed as described below. Migrating cells were identified both from their location on the coverslip and their morphology.

Immunofluorescence Microscopy

For immunofluorescence microscopy, cells were prepared with and without detergent permeabilization before fixation. For permeabilization of cells, coverslips were rinsed, chilled on ice, and then treated with either ice-cold 0.3% Triton-X 100 or 100 μM digitonin in Tris buffer (25 mM, pH 7.4) containing 1 mM PMSF, 10 μg/ml leupeptin, and 10 μg/ml aprotinin for 30 s and then fixed for 20 min with 2% formaldehyde in phosphate-buffered saline (PBS) at room temperature before staining. Alternatively, intact cells were rinsed and directly fixed with 2% formaldehyde (wt/vol) in PBS at room temperature for 20 min before staining.

The staining procedure involved washing coverslips with PBS three times and extracting with −20°C acetone for 30 s. Then the specimens were blocked with 3% serum albumin in PBS for 30 min at 37°C and incubated with primary antibodies (10–20 μg/ml in 3% albumin in PBS) for 1 h at 37°C. After being washed three times with PBS, the cells were incubated with fluorescein-labeled and/or Texas Red-labeled secondary antibodies (Calbiochem, La Jolla, CA) for 1 h at 37°C, washed three times with PBS, and mounted with Vectashield (Vector Laboratories, Burlingame, CA). Immunofluorescence microscopy used a Nikon Microphot-FXA/SA with 60× and 1.4

aperature oil immersion objective, and images were captured and processed as described below.

Three-Dimensional (3D) Image Reconstruction

Fluorescent images of specimens were acquired using a Photometrics AT200 cooled CCD camera (Photometrics, Tucson, AZ). To acquire images at different Z planes of the specimens, the camera was computer controlled in concert with a piezoelectric stepping motor on the microscope objective. The stack of images was stored and processed using CellSCAN data acquisition software. Point spread function was obtained by imaging a through-focus series of optical sections of a 0.2 μm in diameter fluorescein or Texas Red bead (Molecular Probes, Eugene, OR) under identical optical conditions as those used to obtain specimen images. The photons in Z planes above and below the focal plane were reassigned using the point spread function and an algorithm for photon reassignment by the CellSCAN system (Scanalytics, Billercia, MA; Loew *et al.*, 1993). Each Z-axis increment was 0.25–0.5 μm and 15–20 planes were collected and processed for each specimen. Images can be viewed as a montage view of individual Z planes or integrated and restored into a volume image. The images were transferred as data files and printed with Adobe Photoshop version 3.0.

Differential Extraction of Cell Monolayers

CEF cells on a 100-mm polystyrene culture dish were washed twice with TBS, permeabilized with 0.3% Triton X-100 in TBS or in Tris buffer (25 mM, pH 7.4) without NaCl, containing 10 μg/ml leupeptin, 10 μg/ml aprotinin, and 1 mM PMSF for 30 s at room temperature or on ice, and the soluble fraction was collected. The residue of the cells remaining adhered on the dish was washed with TBS or Tris buffer without NaCl twice and extracted with 0.65 M NaCl in Tris buffer for 30 min at room temperature. This cytoskeletal extract was collected and the insoluble cell fraction retained on the dish was washed twice and scraped off with TBS. Each of the three fractions (soluble, cytoskeleton, and insoluble) was normalized by volume and boiled with 2× Laemmli sample buffer for 5 min. The samples were loaded by the same volume and Western blotting was done using mAb against M130, the C5C antibody against myosin, antipeptide antibody against PP1Cα, and antipeptide antibody against PP1Cδ. Samples were stained with secondary fluorescein-labeled antibody and quantitation was done with a Molecular Dynamics (Sunnyvale, CA) FluorImager and ImageQuant software. The percentage of M130 and myosin in the soluble, cytoskeleton, and insoluble fractions was calculated from the total integrated signal of the three samples.

RESULTS

Western Blotting Total Cell Proteins with Antibody Reagents

To demonstrate the specificity of the different antibodies, cells were dissolved in Lamelli sample buffer and the total proteins were immunoblotted. For M130 two different antibodies were used: one was a monoclonal raised against the chicken gizzard 130-kDa subunit of the phosphatase (M130) and the other a polyclonal made by immunizing rabbits with the recombinant N-terminal portion of M130. These both reacted strongly and specifically with proteins that migrated at about 130 kDa in Western blots of total cell proteins (Figure 1, lanes A and B). The M130 subunit exists as multiple isoforms of 130–133 kDa and also is well known to be quite sensitive to proteolytic digestion,

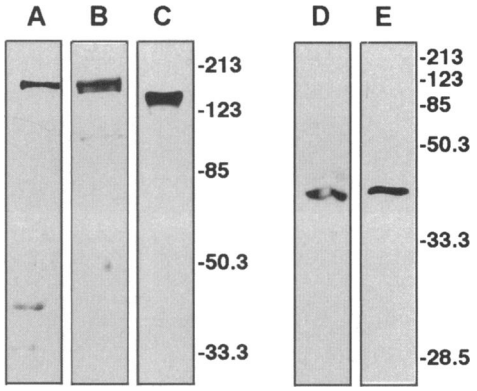

Figure 1. Western blotting of total CEF cell proteins. To show the specificity of antibodies used in this study, CEF cells were scraped from dishes and total cell proteins were separated by SDS-PAGE (10% for lanes A, B, and C; 12% for lanes D and E). Monoclonal mouse antibody against M130 (lane A), rabbit polyclonal antibody against M130 (lane B), sheep polyclonal antibody against MLCK (lane C), rabbit antipeptide antibodies against PP1Cα (lane D), and PP1Cδ (lane E) were used in Western blotting as described in MATERIALS AND METHODS. Similar results were obtained with several cell cultures in independent experiments. Migration of prestained molecular weight markers are shown for myosin heavy chain (213 kDa), galactosidase (123 kDa), bovine serum albumin (85 kDa), ovalbumin (50.3 kDa), carbonic anhydrase (33.3 kDa), and soybean trypsin inhibitor (28.5 kDa).

with fragments of smaller size (especially 58 kDa) observed in purified MLCP as well as in Western blots of tissue extracts (Pato and Kerc, 1985; Alessi *et al.*, 1992; Okubo *et al.*, 1994; Shimizu *et al.*, 1994). The relative lack of immunoreactive fragments of M130 in several different experiments indicated effective inhibition of proteolysis during our sample preparation. There were no proteins detected at the bottom portions of the immunoblots that do not appear in the Figure 1 (i.e., at <30 kDa). Proteins that could have been fragments of the M130 were weakly stained in some Western blots of total cell proteins, but always proteins of approximately 130 kDa were by far the most intensely stained.

Antibodies against PP1Cα and PP1Cδ were made against synthetic peptides corresponding to unique sequences at the C-termini of these proteins. Such antibodies were shown to be specific for the separate isoforms (Villa-Moruzzi *et al.*, 1996) and each reacted with a band at approximately 37 kDa in Western blots of total CEF cell proteins [Figure 1, lanes D (PP1Cα) and E (PP1Cδ)]. For myosin II we used a monoclonal antibody (C5C) that binds the S2 region of myosin, characterized elsewhere (Ito *et al.*, 1989). Another antibody preparation used in this study was a sheep antibody against MLCK that reacted with a single protein of approximately 125 kDa in Western blots of total cell proteins (Figure 1, lane C). Similar results were obtained for both types of cells used in this study, chicken embryo fibroblasts and rat aortic SMCs.

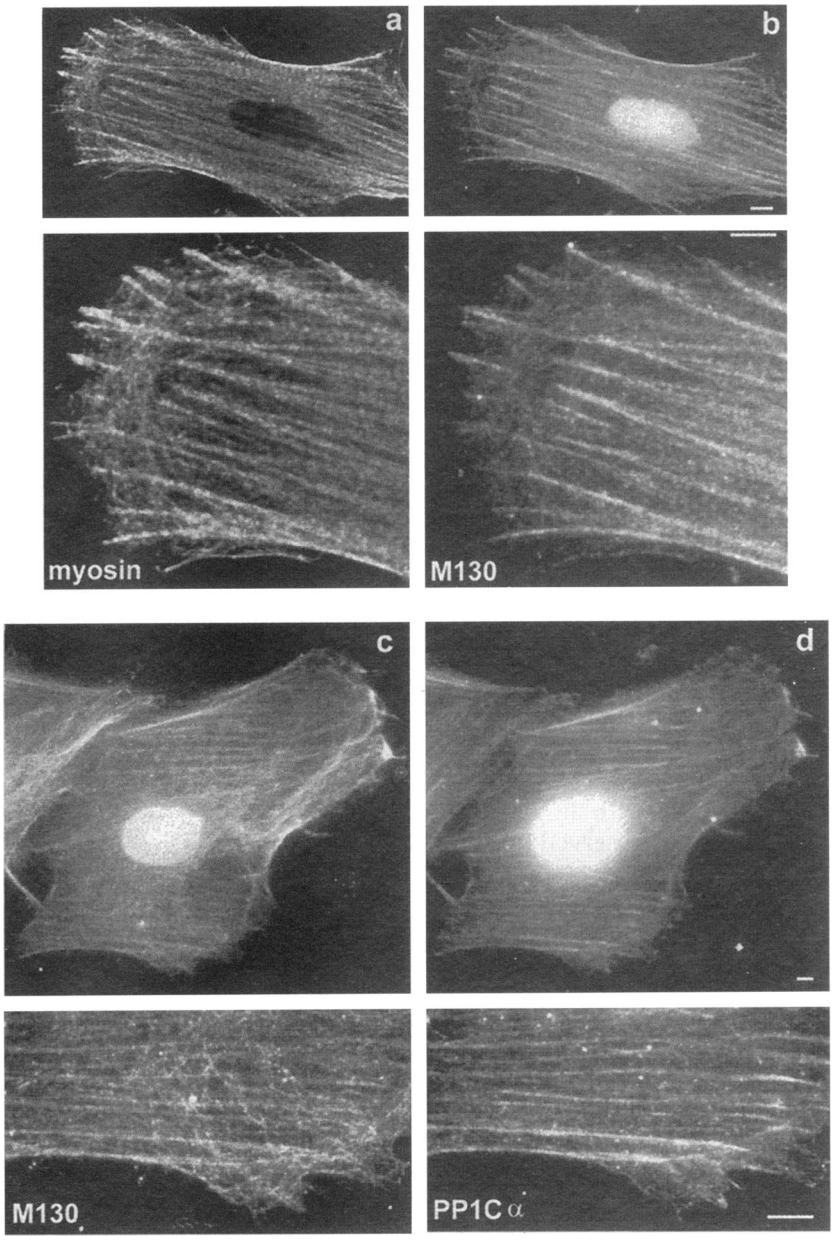

Figure 2. Localization of myosin and MLCP M130 and PP1Cα subunits in rat aortic SMCs. To visualize intracellular distribution of MLCP subunits, cultured SMCs were grown on coverslips, permeabilized, and fixed with formaldehyde before immunofluorescence microscopy with different antibodies, as described in MATERIALS AND METHODS. In the four panels in the top half of the figure, double immunofluorescence staining used monoclonal primary antibody against myosin, with fluorescein secondary antibody (panel a), and rabbit polyclonal primary antibody against M130, with Texas Red secondary antibody (panel b). The images below labeled myosin and M130 are displayed twice as large as the corresponding regions in the top panels. Bars, 5 μm. In the four panels in the bottom half of the figure, double immunofluorescence staining used monoclonal primary antibody against M130, with fluorescein secondary antibody (panel c), and rabbit polyclonal antipeptide primary antibody against PP1Cα, with Texas Red secondary antibody (panel d). The images below labeled M130 and PP1Cα are displayed three times as large as the corresponding regions in the top panels. Bars, 5 μm. The images were captured with a cooled CCD camera at exposure times of 0.5–2 s and processed through Adobe Photoshop. Incubation with either secondary antibody, without primary antibody incubation, gave low backgrounds that appeared blank. Results were replicated with different cell cultures in several independent experiments.

Subcellular Localization of Myosin and Phosphatase Subunits M130 and PP1C in Rat Aorta SMC

Myofibrils from smooth muscle have been used as a source for MLCP, that has been purified as a heterotrimer of a myosin-binding subunit (M130), plus a 20-kDa subunit, plus the δ isoform of PP1C. Using cultured rat aorta SMCs, we examined the distribution of myosin, M130, and the PP1C subunit isoforms. Double staining of rat aorta SMCs permeabilized briefly before fixation showed colocalization of myosin (Figure 2a) and the M130 subunit of the phosphatase (Figure 2b), with both concentrated along stress fibers. There was staining of the nucleus for M130, not for myosin. Closer examination (Figure 2, a and b, bottom panels) revealed that the staining for both myosin and M130 was mostly concentrated on the stress fibers, but there also was specific staining for myosin that resembled a tangle of fine fibers in a swath across the cell near, but not at, the edge of the cell. Also noticeable in these panels, the staining of the stress fibers for M130 appeared to be continuous, whereas myosin staining appeared to be banded or striped along the fibers. In other experiments, staining with fluorescein-phalloidin gave distinctive, brilliant stress fiber staining, and double staining (Texas Red)

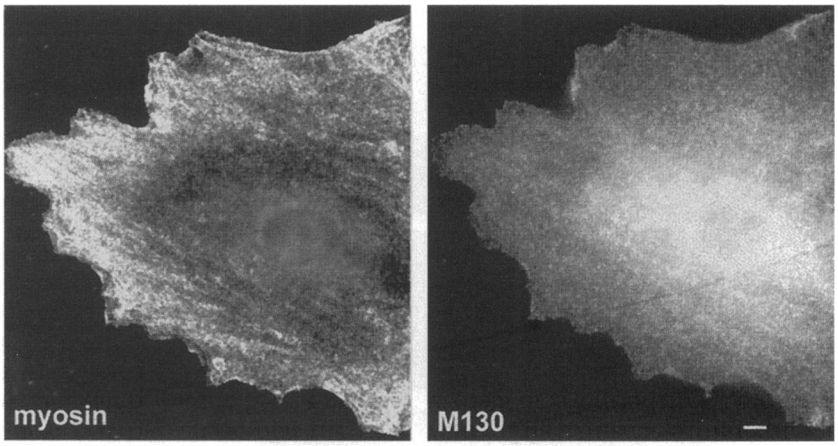

Figure 3. Colocalization of myosin and M130 of MLCP in nonpermeabilized rat aorta SMCs. Cells were grown on coverslips and directly fixed with formaldehyde, without prior permeabilization, before immunofluorescence microscopy with different antibodies, as described in MATERIALS AND METHODS. Double immunofluorescence staining used monoclonal primary antibody against myosin II, with fluorescein secondary antibody (left panel), and rabbit polyclonal primary antibody against M130, with Texas Red secondary antibody (right panel). Bar, 5 μm.

for M130 showed its concentration along these stress fibers. This was the same in either SMC or CEF cells. Importantly, both the monoclonal and polyclonal anti-M130 antibodies gave identical results. In the course of this study, we discovered that the distribution of M130 was sensitive to conditions used for permeabilization (see below). The conditions used for the experiments depicted in Figure 2 (on ice, no NaCl) gave the maximum retention of M130 in the specimens after permeabilization.

Alternatively, with intact nonpermeabilized cells double staining for myosin and M130 (Figure 3) did not reveal prominent staining of stress fibers and showed an intracellular distribution somewhat different for each protein. Staining for myosin was brightest near the perimeter of the cells, with little signal from the center or the perinuclear area of the cells. There was the suggestion of a fibrillar staining pattern that was partially obscured by diffusely granular staining. The intense staining for myosin near the perimeter of the cells was reminiscent of the clusters of short fibers seen in Figure 2a. Compared with this distribution of myosin in nonpermeabilized cells, staining for M130 was not in a fibrillar pattern. Instead, M130 appeared to be diffusely granular throughout the cell, with staining intensity that increased from the perimeter of the cell toward the perinuclear area, which was the brightest portion of the image. These results show that most of the myosin and M130 in cells are not distributed together. The M130 staining appeared as one would expect for a soluble cytoplasmic protein. Therefore, despite the colocalization of myosin and M130 on stress fibers in Figure 2 and the biochemical purification of MLCP that depends on its binding to myosin, there seems to be a significant cytoplasmic pool of M130.

Another integral subunit of purified MLCP, the δ isoform of PP1C, did not colocalize with either M130 or myosin in permeabilized cells. In permeabilized cells it was the PP1Cα isoform, not PP1Cδ, that colocalized with M130 by double staining (Figure 2, c and d). Closer examination (Figure 2, c and d, bottom panels) showed the coincident staining for M130 and PP1Cα on stress fibers. The same results were obtained with nonmuscle CEF cells. Previous reports had shown PP1C association with microfilaments in rat embryo fibroblasts (REF52 cells; Fernandez *et al.*, 1990). In permeabilized cells, PP1Cδ was found only within the nucleus. In cells fixed without permeabilization, staining for PP1Cδ was concentrated in the nucleus, but there also was staining at the periphery of the cell, concentrated in distinctive streaks emanating from the edge of the cell (Figure 4). Double immunofluorescence staining for focal adhesion kinase (FAK) and for PP1Cδ gave the same patterns (Figure 4, see bottom panels), indicative of localization of PP1Cδ in focal adhesions.

Differential Extraction of Myosin and M130 from Cells

Because localization of M130 in nonpermeabilized cells appeared to be cytoplasmic (Figure 3), we examined the subcellular distribution of myosin II, and the M130 and PP1C subunits of MLCP by differential extraction of cells. Cells were permeabilized briefly and soluble, cytoskeletal, and insoluble fractions prepared as described in MATERIALS AND METHODS. The same results were obtained in experiments using either Triton X-100 or digitonin permeabilization. At room temperature, with detergent in saline, essentially all of the M130, PP1Cα, and PP1Cδ were recovered in the soluble fraction. About two-thirds of myosin was recovered in the soluble fraction, though it also was extracted with 0.65 M NaCl from the cytoskeleton remaining after permeabilization. Myosin was detected in the insoluble fraction after detergent and salt extraction as well. The relative distribution of M130 and myosin in the different fractions was compared with cells treated at room temperature or on ice, with

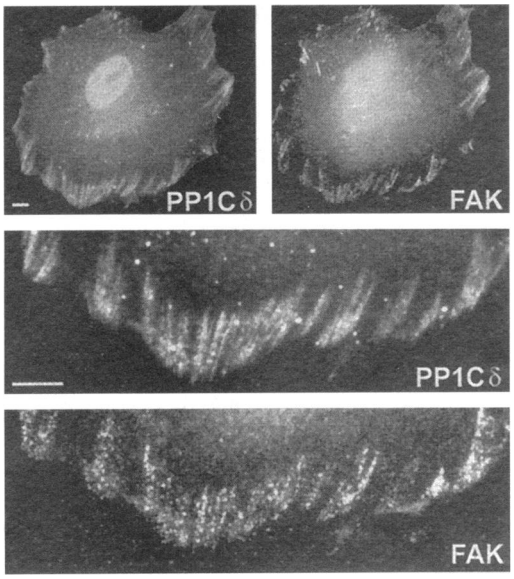

Figure 4. Localization of PP1Cδ and FAK in rat aortic SMCs. To visualize the distribution of PP1Cδ in SMCs, cells were grown on coverslips and fixed with 2% formaldehyde without permeabilization before immunofluorescence microscopy was performed as described in MATERIALS AND METHODS. Double immunofluorescence staining used rabbit antipeptide primary antibody against PP1Cδ, with fluorescein secondary antibody (top left and middle panels), and monoclonal primary antibody against FAK, with Texas Red secondary antibody (top right and bottom panels). The PP1Cδ and FAK were concentrated into foci near the periphery of the cell. Portions of the cells are shown three times larger in the middle and bottom panels for comparison. Images were captured with a cooled CCD camera, with exposure times of 0.2–2 s. Incubation of cells with only secondary antibodies gave low background that appeared blank. Results were replicated with different cell cultures in several independent experiments. Bars, 5 μm.

saline or no added NaCl in the permeabilization solution (Table 1). Omitting NaCl from the permeabilization solution reduced considerably the proportion of M130 and myosin in the soluble fraction. Chilling cells on ice also reduced the amount of M130 in the soluble fraction, yielding as much as 40% of the M130 in the cytoskeletal fraction. These were the conditions used to prepare samples shown in Figure 2. Under all of the various conditions of permeabilization tested here, the PP1Cα and the PP1Cδ were essentially all (>90%) in the soluble fraction. The difference in the distribution of M130 was not due to less proteolysis of M130 at the lower temperature, based on Western blotting of the fractions. There also was not a significant change in the pattern of proteins stained by Coomassie blue in the various fractions when cell monolayers were extracted on ice compared with those extracted at room temperature. The effect of temperature on the distribution of M130 was observed with both CEFs and SMCs and was reproduced in three independent experiments. Although MLCP is cytoplasmic by immunofluorescence (Figure 3) and soluble by permeabilization (Table 1), it has been purified with myofibrils in the particulate fraction after homogenization of smooth muscle tissue (Pato and Kerc, 1985; Alessi *et al.*, 1992; Okubo *et al.*, 1993; Shimizu *et al.*, 1994; Shirazi *et al.*, 1994). Our results show that the chilling of cells (or tissues) on ice promotes the association of MLCP with the cytoskeleton (or myofibrils) and this may account for its effective purification as a myosin-associated protein.

Myosin and M130 Localized on the Tailing Edge of Migrating Cells

In a wound-healing model, fibroblasts are scraped from a region of a coverslip and the remaining cells migrate into the vacant area. These migrating fibroblasts take on a fan-shaped morphology, with a broad leading edge of lamellipodia and a narrow tailing edge. Within these migrating CEFs, the M130 subunit of MLCP was distributed in a distinctive pattern quite different from myosin II in the same cells and was different compared with M130 in nonmigrating cells. There was a concentration of M130 in the rear of the cell and it was depleted from the front, or leading

Table 1. Distribution of myosin and MLCP-M130 by differential extraction[a]

	Room temperature						On ice					
	Saline			No NaCl			Saline			No NaCl		
	Soluble	Cytoskeleton	Insoluble	Soluble	Cytoskeleton	Insoluble	Soluble	Cytoskeleton	Insoluble	Soluble	Cytoskeleton	Insoluble
M130	100	nd	nd	72	28	nd	59	41	nd	62	38	nd
myosin	71	19	10	44	30	26	64	4	32	84	8	8

[a]The distribution of myosin, M130, and PP1C isoforms in the soluble, cytoskeleton, and insoluble fractions were determined by differential extraction of cells and quantitative immunoblotting of samples as described in MATERIALS AND METHODS. The total of the three fractions from each condition was taken as 100% and used to calculate the distribution. For some samples, no staining above background was detected, and these are indicated as nd, not detected. Essentially, all of the PP1Cα and PP1Cδ were in the soluble fraction under all conditions.

edge, of the cell to the point that no staining was visualized. Using 3D image reconstruction and double immunofluorescence staining of nonmigrating CEFs that were outside the wound and did not exhibit the fan-shaped morphology, the highest intensity staining for both myosin II and M130 was at the perimeter of the cells (Figure 5A, panels a and b). There also was staining within the cells that appeared to be punctate, but aligned in rows that probably correspond to the stress fibers.

Migrating CEFs were stained by double immunofluorescence staining, and 3D image reconstruction showed distribution of myosin (Figure 5A, panel c) in a lacework pattern in the leading half of the cell (white arrow indicates direction of migration) and concentrated staining on the edges of the cell and in the tail area (upper left corner of Figure 5A, panel c). On the other hand, the M130 subunit of MLCP was not detected in the leading half of migrating CEFs (Figure 5A, panel d), where there obviously was myosin II present. The M130 was present in a punctate cytoplasmic pattern in the rear half of the cell, a pattern like in a nonmigrating cell (compare Figure 5A, panel b and 5A, panel d), and was concentrated in the tailing edge. From these images one sees that MLCP was concentrated with myosin II in the tailing edge, but was excluded from the leading portion of migrating CEF cells where myosin II was present, albeit in a different pattern.

In contrast to this selective distribution of MLCP M130 subunit, the myosin kinase MLCK was distributed throughout migrating cells (Figure 5B). A separate image is shown for staining of MLCK because this was done with methanol-fixed cells. The anti-MLCK did not work with formalin-fixed cells and anti-M130 was not effective with methanol-fixed cells, precluding double labeling with these antibodies. Regardless, the results show that MLCP and myosin kinase are distributed independently within cells.

The concentration of the M130 subunit of MLCP and myosin II at the tailing edge of migrating CEFs was examined in many cells using the CellSCAN microscopy system. A montage of individual Z plane-restored images revealed the concentration of M130 into a 3D cone of puncta that seemed aligned on fibers, coalescing at the tailing edge of CEF cells (Figure 6A). The nucleus of the cell is faintly visible in the center, for orientation. The tailing edge appears at the top of the frames and leading edge

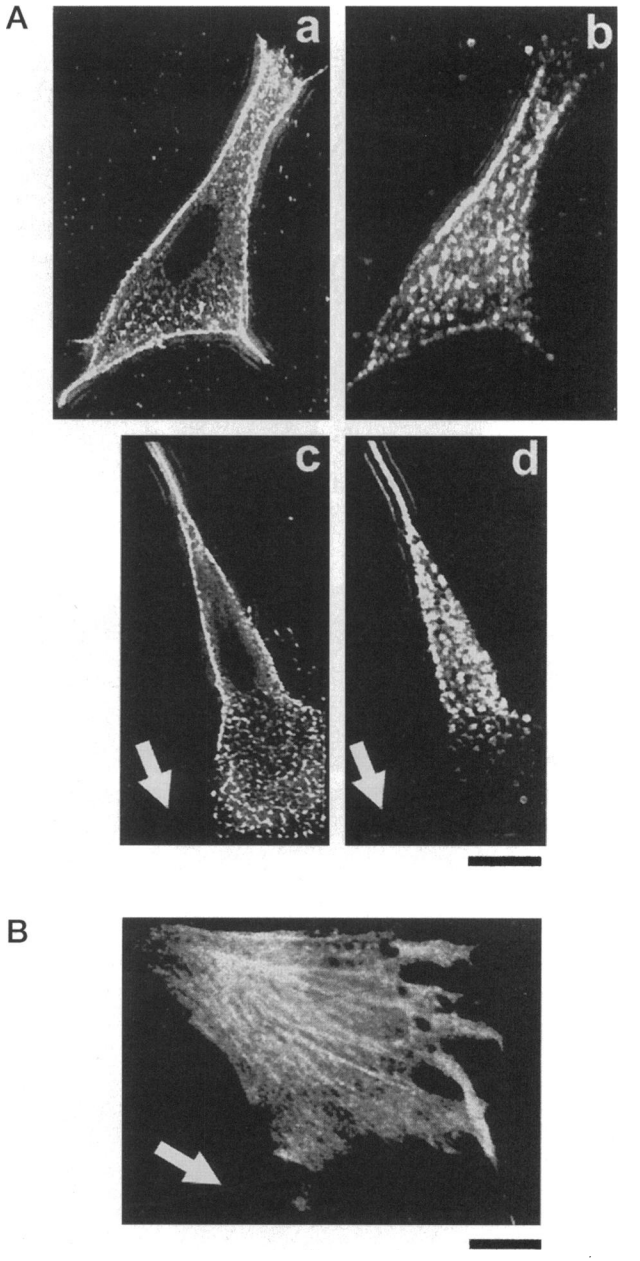

Figure 5 (cont). followed by fluorescein-labeled antimouse antibody for myosin (panels a and c) and Texas Red-labeled anti-rabbit antibody for M130 (panels b and d). Fluorescence was not detected through the opposite filters when specimens were singly stained in a test for bleed-through emission. Controls omitting primary antibody gave background staining that appeared blank at these exposures. Different Z-axis plane images were collected with a CCD camera and processed by photon reassignment (CellSCAN system) as described in MATERIALS AND METHODS. The images shown are processed as volume display and are representative of the cell populations in multiple specimen preparations. Bar, 20 μm. (B) Migrating CEFs were fixed with −20°C methanol and stained with sheep antibody against MLCK followed by fluorescein-labeled antisheep antibody. The image was taken with a CCD camera but not processed by photon reassignment. Bar, 20 μm.

Figure 5. Distribution of myosin, M130, and MLCK in adherent and migrating CEFs. (A) A nonmigrating CEF (panels a and b) and a migrating cell (panels c and d) were permeabilized with 0.3% Triton X-100 for 30 s at room temperature and fixed with 2% formaldehyde. Double staining used mouse monoclonal antibody against myosin and rabbit polyclonal antibody against M130

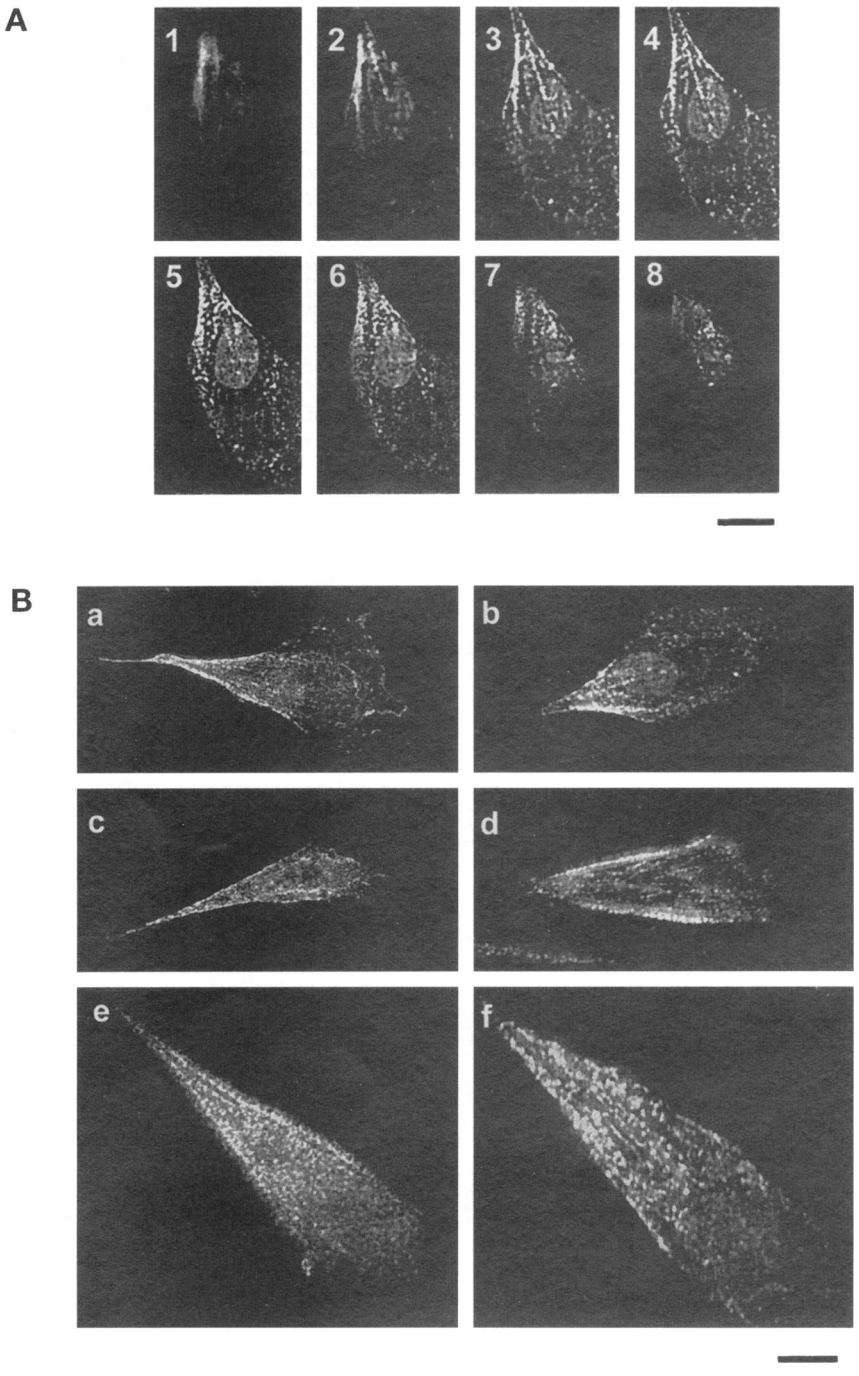

Figure 6. Reconstructed 3D images of M130 in migrating CEFs. (A) Montage of Z plane images of M130 in migrating CEFs starting from the substratum (panel 1) to the apex of the cell (panel 8). The CEFs were permeabilized with 0.3% Triton X-100, fixed with 2% formaldehyde, and stained with monoclonal antibody against M130 followed by fluorescein-labeled secondary antibody. Images were taken with a CCD camera and processed by CellSCAN photon reassignment using an experimentally determined point spread function. Every other plane of 16 images taken at 0.25-μm Z-axis increments is shown. Bar, 20 μm. (B) Volume display of the distribution of M130 in migrating CEFs as processed by photon reassignment using CellSCAN software. CEFs were directly fixed with 2% formaldehyde without prior permeabilization (panels a, c, and e) or were permeabilized with 0.3% Triton X-100 before formaldehyde fixation (panels b, d, and f). The cells were stained with monoclonal antibody against M130 (panels a–d) or rabbit polyclonal antibody against M130 (panels e and f) followed by fluorescein-labeled secondary antibodies. Images were taken with a CCD camera and processed using CellSCAN photon reassignment software. Volume displays were created from 15–20 planes at 0.25–0.50-μm Z-axis increments, as described in MATERIALS AND METHODS. As a specific example, the image in panel b is the volume display made from the multiple images in Figure 6A. The images are representative of the cell populations in multiple specimen preparations. Bar, 20 μm.

toward the bottom. The series of images 1 through 8 are every other Z plane from a stack of 16. The view of the entire assembled stack of Z planes for this particular cell is shown in Figure 6B, panel b. Dozens of migrating CEF cells were analyzed by immunofluorescence and CellSCAN 3D image restoration. Several of these individual cells are shown as full stack images in Figure 6B.

DISCUSSION

Distribution of Myosin and MLCP

MLCP has been purified from smooth muscle tissue as an enzyme tightly bound to myofibrils (Pato and Kerc, 1985; Alessi *et al.*, 1992; Shimizu *et al.*, 1994; Shirazi *et al.*, 1994). Therefore, one might have predicted that MLCP would be distributed within cells like myosin

and primarily be bound to stress fibers. Indeed, cells briefly permeabilized with detergent before fixation and double stained for myosin and the M130 subunit of MLCP showed staining coincident with stress fibers. However, close examination revealed there was a swath across the edge of the cell that stained selectively for myosin. Differential distribution of myosin and MLCP was even more obvious in migrating cells. Here, the cells were stained for myosin II in both the leading and tailing halves of the cell in different patterns. But, the leading half of cells was devoid of staining for MLCP M130, whereas the tailing half was brightly stained for M130 in a distinctive pattern visualized using CellSCAN 3D image reconstruction. The results show that MLCP does not always colocalize with myosin II and imply that there are mechanisms for control of M130 distribution within cells.

Immunofluorescence microscopy of cells fixed without permeabilization showed there was substantial cytoplasmic staining for M130. This led us to examine the distribution of M130 and myosin II by Western immunoblotting of fractions prepared by differential extraction of cell monolayers. Permeabilization with either Triton X-100 or digitonin to release a soluble fraction, followed by salt extraction of the cytoskeleton, showed cytoplasmic and cytoskeletal pools of MLCP. Interestingly, the distribution between these pools was quite sensitive to conditions used for permeabilization, especially temperature. The results show that the MLCP readily dissociates from the cytoskeleton in SMCs and fibroblasts and by inference from myofibrils in smooth muscle tissue. The conditions of extraction, and presumably different physiological circumstances, affect the distribution of MLCP.

Recently, affinity chromatography in the presence of Mg-ATP showed that M130 bound to phosphorylated, but not dephosphorylated myosin. In the absence of Mg-ATP, however, M130 bound to both phosphorylated and dephosphorylated myosin (Ichikawa *et al.*, 1996a). These binding assays are consistent with our observation that in intact cells containing mM ATP a considerable fraction of MLCP is cytosolic. In contrast, purification of MLCP from tissue involved homogenization in ice-cold buffers with chelators to remove Mg^{2+}. These conditions would be expected to promote binding of M130 to both phosphorylated and unphosphorylated myosin. The marked effect of temperature we observed on the distribution of M130 could in part be due to the extreme temperature dependence of MLCP activity, with a Q_{10} of 5 (Mitsui *et al.*, 1994). A large decrease in the activity of the phosphatase upon chilling of cells might enhance binding to the cytoskeleton by reducing dephosphorylation of MLC20. There has been a question of how MLCP could work if it was tightly bound to myosin that was present in a substantial molar excess over the phosphatase (Alessi *et al.*, 1992). The preferential binding of cytoplasmic MLCP to phosphorylated myosin II (its substrate) could account for how MLCP efficiently carries out dephosphorylation of intracellular myosin.

Distribution of PP1C Isoforms on Stress Fibers or in Focal Adhesions

MLCP purified from smooth muscle myofibrils contains the catalytic subunit of type 1 protein phosphatase, PP1C. Specific antibodies and amino acid sequencing of tryptic peptides showed the PP1 catalytic subunit was the δ isoform (Alessi *et al.*, 1992; Okubo *et al.*, 1994; Shimizu *et al.*, 1994). Based on these results, PP1Cδ has been considered to be the catalytic subunit of MLCP. However, M130 can bind to α, γ, and δ PP1C isoforms in vitro (Chen *et al.*, 1994b). We found with double staining colocalization of M130 and PP1Cα on stress fibers. Under the same conditions, PP1Cδ was not localized on stress fibers. This at least raises the possibility that MLCP contains either α or δ PP1C subunits. Most of the MLCP was soluble, and this fraction may contain PP1Cδ, whereas the fraction of MLCP bound to stress fibers could contain PP1Cα. Alternatively, during the enzyme purification an exchange of catalytic subunits might occur, with PP1Cδ recovered along with M130.

Immunofluorescence staining of PP1Cδ in SMC was quite interesting because it colocalized with FAK, which is concentrated in focal adhesions. This may be a specialized targeting site for the PP1Cδ isoform. The M130 did not appear at these sites, suggesting that another targeting subunit for PP1Cδ is involved. There are a number of potential substrates for PP1C in focal adhesions, for example, there is evidence of rapid dephosphorylation of talin by PP1C (Murata *et al.*, 1995). The localization of PP1Cδ within focal adhesions deserves further attention.

Localization of MLCP in Migrating Fibroblasts

For fibroblast migration rear release is proposed for one of the mechanisms (reviewed in Stossel, 1993; Huttenlocher *et al.*, 1995; Lauffenburger and Horwitz, 1996). Mechanisms for this release include cytoskeletal contraction or tension (Jay *et al.*, 1995). Myosin II was found concentrated on the tailing edge, but not organized into filaments in the lamellipodia. Our observations of myosin distribution in migrating cells are consistent with those reported earlier (Conrad *et al.*, 1993; Kolega and Taylor, 1993). Myosin has been localized in the tailing peripheral edge of migrating cells (Kelley *et al.*, 1996). Our results show that M130 likewise was concentrated in the tailing edge of migrating cells (Figures 5A and 6). In migrating fibroblasts, MLC20 on the tailing edge also was shown to be phosphorylated using a fluorescent biosensor specific for phosphorylated myosin (Post *et al.*, 1995). MLC20 phosphorylation was lowest near the leading edge

and highest in the tailing edge of migrating cells. Together these results predict that M130 and phosphorylated myosin II are localized together in the tailing edge. But this presents an apparent contradiction, with the MLCP localized where phosphorylation of MLC20 is the highest. The implication is that the MLCP must be maintained in a low activity form on the tailing edge, probably by phosphorylation of the M130 subunit (see below).

The low molecular weight G-protein, rhoA, has been demonstrated to be functionally linked to the actin cytoskeleton (reviewed in Hall, 1994; Machesky and Hall, 1996; Takai *et al.*, 1996). Inactivation of rho induced cytoskeletal breakdown and inhibited cellular migration (Miura *et al.*, 1993). Contraction of fibroblasts was shown to be induced in response to lysophosphatidic acid or microinjection of activated rhoA (Chrzanowska-Wodnicka and Burridge, 1996). Other data were accumulated using skinned smooth muscle strips to show that MLCP can be inhibited through a rho pathway (Kitazawa *et al.*, 1991; Hirata *et al.*, 1992; Somlyo and Somlyo, 1994; Gong *et al.*, 1996). Inhibition of MLCP by rho also was shown with cultured vascular SMCs (Noda *et al.*, 1995). Phosphorylation of M130 was shown to inhibit phosphatase activity in skinned muscle (Trinkle-Mulcahy *et al.*, 1995). The activity of MLCP also is regulated by phosphorylation of a threonine residue in M130 in vitro (Ichikawa *et al.*, 1996b). More recently, MLCP was inhibited by rhoA binding and by phosphorylation catalyzed by rhoA kinase in fibroblasts (Kimura *et al.*, 1996). We envision that the phosphorylated, inhibited form of MLCP is localized in the tailing edge of migrating fibroblasts by its binding to phosphorylated myosin II.

ACKNOWLEDGMENTS

We thank Dr. Masaaki Ito for providing polyclonal anti-M130 antibody, Dr. J. Thomas Parsons for providing CEF cells and anti-FAK antibody (2A7), Dr. Gary Owens for providing rat aortic SMCs, Dr. Mayumi Hirano for helpful comments, Ron Pace for technical assistance, and Christine Palazzolo for assistance in preparation of the manuscript. We acknowledge the helpful comments of Drs. Avril V. Somlyo and Keith Burridge on drafts of this manuscript. Kohei Murata was supported by a Postdoctoral Fellowship from the American Heart Association, Virginia Affiliate, Inc. The research was supported in part by grant MCB 9505499 from the National Science Foundation to D.L.B. and National Institutes of Health grants HL-23615 and HL-20984 to D.J.H. Facilities were provided by support from the University of Virginia Molecular Biology Institute and the Lucille P. Markey Charitable Trust.

REFERENCES

Alessi, D., MacDougall, L.K., Sola, M.M., Ikebe, M., and Cohen, P. (1992). The control of protein phosphatase-1 by targeting subunits. The major MLCP in avian smooth muscle is a novel form of protein phosphatase-1. Eur. J. Biochem. *210*, 1023–1035.

Chen, Y.H., Chen, M.X., Alessi, D.R., Campbell, D.G., Shanahan, C., Cohen, P., and Cohen, P.T. (1994a). Molecular cloning of cDNA encoding the 110 kD and 21 kD regulatory subunits of smooth muscle protein phosphatase 1M. FEBS Lett. *356*, 51–55.

Chen, Y.H., Hansen, L., Chen, M.X., Bjorbaek, C., Vestergaard, H., Hansen, T., Cohen, P.T., and Pedersen, O. (1994b). Sequence of the human glycogen-associated regulatory subunit of type 1 protein phosphatase and analysis of its coding region and mRNA level in muscle from patients with NIDDM. Diabetes *43*, 1234–1241.

Chrzanowska-Wodnicka, M., and Burridge, K. (1996). Rho-stimulated contractility drives the formation of stress fibers and focal adhesions. J. Cell Biol. *133*, 1403–1415.

Conrad, P.A., Giuliano, K.A., Fisher, G., Collins, K., Matsudaira, P.T., and Taylor, D.L. (1993). Relative distribution of actin, myosin I, and myosin II during the wound healing response of fibroblasts. J. Cell Biol. *120*, 1381–1391.

Fernandez, A., Brautigan, D.L., Mumby, M., and Lamb, N.J. (1990). Protein phosphatase type-1, not type-2A, modulates actin microfilament integrity and myosin light chain phosphorylation in living nonmuscle cells. J. Cell Biol. *111*, 103–112.

Gong, M.C., Fuglsang, A., Alessi, D., Kobayashi, S., Cohen, P., Somlyo, A.V., and Somlyo, A.P. (1992). Arachidonic acid inhibits myosin light chain phosphatase and sensitizes smooth muscle to calcium. J. Biol. Chem. *267*, 21492–21498.

Gong, M.C., Iizuka, K., Nixon, G., Browne, J.P., Hall, A., Eccleston, J.F., Sugai, M., Kobayashi, S., Somlyo, A.V., and Somlyo, A.P. (1996). Role of guanine nucleotide-binding proteins—ras-family or trimeric proteins or both—in Ca^{2+} sensitization of smooth muscle. Proc. Natl. Acad. Sci. USA *93*, 1340–1345.

Hall, A. (1994). Small GTP-binding proteins and the regulation of actin cytoskeleton. Annu. Rev. Cell Biol. *10*, 31–54.

Hirata, K., Kikuchi, A., Sasaki, T., Kuroda, S., Kaibuchi, K., Matsuura, Y., Seki, H., Saida, K., and Takai, Y. (1992). Involvement of rho p21 in the GTP-enhanced calcium ion sensitivity of smooth muscle contraction. J. Biol. Chem. *267*, 8719–8722.

Huttenlocher, A., Sandborg, R.R., and Horwitz, A.F. (1995). Adhesion in cell migration. Curr. Opin. Cell Biol. *7*, 697–706.

Ichikawa, K., Hirano, K., Ito, M., Tanaka, J., Nakano, T., and Hartshorne, D.J. (1996a). Interaction and properties of smooth muscle MLCP. Biochemistry *35*, 6313–6320.

Ichikawa, K., Ito, M., and Hartshorne, D.J. (1996b). Phosphorylation of the large subunit of MLCP and inhibition of phosphatase activity. J. Biol. Chem. *271*, 4733–4740.

Ito, M., Pierce, P.R., Allen, R.E., and Hartshorne, D.J. (1989). Effect of monoclonal antibodies on the properties of smooth muscle myosin. Biochemistry *28*, 5567–5572.

Jay, P.Y., Pham, P.A., Wong, S.A., and Elson, E.L. (1995). A mechanical function of myosin II in cell motility. J. Cell Sci. *108*, 387–393.

Kelley, C.A., Sellers, J.R., Gard, D.L., Bui, D., Adelstein, R.S., and Baines, I.C. (1996). *Xenopus* nonmuscle myosin heavy chain isoforms have different subcellular localization and enzymatic activities. J. Cell Biol. *134*, 675–687.

Kimura, K., Ito, M., Amano, M., Chihara, K., Fukata, Y., Nakafuku, M., Yamamori, B., Feng, J., Nakano, T., Okawa, K., Iwamatsu, A., and Kaibuchi, K. (1996). Regulation of MLCP by rho and rho-associated kinase (rho-kinase). Science *273*, 245–248.

Kitazawa, T., Masuo, M., and Somlyo, A.P. (1991). G protein-mediated inhibition of myosin light-chain phosphatase in vascular smooth muscle. Proc. Natl. Acad. Sci. USA *88*, 9307–9310.

Kolega, J., and Taylor, D.L. (1993). Gradients in the concentration and assembly of myosin II in living fibroblasts during locomotion and fiber transport. Mol. Biol. Cell *4*, 819–836.

Lauffenburger, D.A., and Horwitz, A.F. (1996). Cell migration—a physically integrated molecular process. Cell *84*, 359–369.

Loew, L.M., Tuft, R.A., Carrington, W., and Fay, F.S. (1993). Imaging in five dimensions: time-dependent membrane potentials in individual. Biophys. J. *65*, 2396–2407.

Machesky, L.M., and Hall, A. (1996). Rho: a connection between membrane receptor signalling and the cytoskeleton. Trends Cell Biol. *6*, 304–310.

Mitsui, T., Kitazawa, T., and Ikebe, M. (1994). Correlation between high temperature dependence of smooth muscle myosin light chain phosphatase activity and muscle relaxation rate. J. Biol. Chem. *269*, 5842–5848.

Miura, H., Kikuchi, A., Musha, T., Kuroda, S., Yaku, M., Sasaki, S., and Takai, Y. (1993). Regulation of morphology by rho p21 and its inhibitory GDP/GTP exchange protein (rho GD1) in Swiss 3T3 cells. J. Biol. Chem. *268*, 510–515.

Murata, K., Sakon, M., Kambayashi, J., Okuyama, M., Hase, T., and Mori, T. (1995). Platelet talin is phosphorylated by calyculin A. J. Cell. Biochem. *57*, 120–126.

Noda, M., Yasuda-Fukazawa, C., Moriishi, K., Kato, T., Okuda, T., Kurokawa, K., and Takuwa, Y. (1995). Involvement of rho in GTP gamma S-induced enhancement of phosphorylation of 20 kD myosin light chain in vascular smooth muscle cells: inhibition of phosphatase activity. FEBS Lett. *367*, 246–250.

Okubo, S., Erdodi, F., Ito, M., Ichikawa, K., Konishi, T., Nakano, T., Kawamura, T., Brautigan, D.L., and Hartshorne, D.J. (1993). Characterization of a myosin-bound phosphatase from smooth muscle. Adv. Prot. Phosphatases *7*, 295–314.

Okubo, S., Ito, M., Takashiba, Y., Ichikawa, K., Miyahara, M., Shimizu, H., Konishi, T., Shima, H., Nagao, M., and Hartshorne, D.J. (1994). A regulatory subunit of smooth muscle myosin bound phosphatase. Biochem. Biophys. Res. Commun. *200*, 429- 434.

Pato, M.D., and Kerc, E. (1985). Purification and characterization of a smooth muscle MLCP from turkey gizzards. J. Biol. Chem. *260*, 12359–12366.

Post, P.L., DeBiasio, R.L., and Taylor, D.L. (1995). A fluorescent protein biosensor of myosin II regulatory light chain phosphorylation reports a gradient of phosphorylated myosin II in migrating cells. Mol. Biol. Cell *6*, 1755–1768.

Shimizu, H., Ito, M., Miyahara, M., Ichikawa, K., Okubo, S., Konishi, T., Naka, M., Tanaka, T., Hirano, K., and Hartshorne, D.J. (1994). Characterization of the myosin-binding subunit of smooth muscle MLCP. J. Biol. Chem. *269*, 30407–30411.

Shirazi, A., Iizuka, K., Fadden, P., Mosse, C., Somlyo, A.P., Somlyo, A.V., and Haystead, T.A. (1994). Purification and characterization of the mammalian myosin light chain phosphatase holoenzyme. The differential effects of the holoenzyme and its subunits on smooth muscle. J. Biol. Chem. *269*, 31598–31606.

Somlyo, A.P., and Somlyo, A.V. (1994). Signal transduction and regulation in smooth muscle (published erratum appears in Nature *372*, 812, 1994). Nature *372*, 231–236.

Stossel, T.P. (1993). On the crawling of animal cells. Science *260*, 1086–1094.

Takai, Y., Sasaki, T., Tanaka, K., and Nakanishi, H. (1996). Rho as a regulator of the cytoskeleton. Trends Biol. Sci. *20*, 227–231.

Trinkle-Mulcahy, L., Ichikawa, K., Hartshorne, D.J., Siegman, M.J., and Butler, T.M. (1995). Thiophosphorylation of the 130-kD subunit is associated with a decreased activity of myosin light chain phosphatase in alpha-toxin-permeabilized smooth muscle. J. Biol. Chem. *270*, 18191–18194.

Villa-Moruzzi, E., Puntoni, F., and Marin, O. (1996). Activation of protein phosphatase-1 isoforms and glycogen synthase kinase-3-beta in muscle from mdx mice. Int. J. Biochem. Cell Biol. *28*, 13–22.